

Full Length Article

Comparative study of laser induced periodic surface structures formed on pulsed laser deposited and magnetron sputtered titanium oxide films

A. Talbi^a, P. Coddet^a, M. Tabbal^b, A.L. Thomann^a, E. Millon^a, A. Stolz^a, C. Boulmer-Leborgne^a, G.M. O'Connor^c, N. Semmar^{a,*}^a GREMI, UMR 7344 CNRS / Université d'Orléans, 14 rue d'Issoudun, B.P. 6744, 45067 Orléans Cedex 2, France^b Department of Physics, American University of Beirut, Bliss St. P.O. Box 11-0236, Riad el Solh, Beirut 1107 2020, Lebanon^c NCLA/Inspire Laboratories, School of Physics, National University of Ireland Galway, University Road, Galway, Ireland

ARTICLE INFO

Keywords:

LIPSS
Nanostructuring
Pulsed laser deposition
Magnetron sputtering
Titanium oxide thin films
Femtosecond laser

ABSTRACT

In this paper, we present a comparative study of LIPSS formation on sub-stoichiometric titanium oxide thin films grown using pulsed laser deposition (PLD) and Magnetron Sputtering (MS). Irradiation was performed using femtosecond lasers beams, emitting at wavelengths 266 and 1030 nm, and at different numbers of laser pulses and laser fluences. Conditions for the formation of LIPSS were determined for both types of films, at 266 nm. A variety of nanostructures such as LSFL, HSFL, spikes, dots were detected and their shapes and sizes were found to strongly depend on laser fluence and number of pulses, as essentially dictated by free-surface energy minimization. LIPSS appeared to follow similar formation pattern for both PLD and MS films, except for some delamination detected for the MS films. This was attributed to better adhesion and a lower stress state of the PLD films compared to their MS counterparts. Large surface nanostructuring experiments performed at 1030 nm showed less delamination with the increase of the laser fluence, resulting from a competition between the cracking and the melting of the layers.

1. Introduction

Laser irradiation of materials offers a direct one-step route to induce micro and nano-structures on a variety of solid surfaces in view of tailoring their properties for specific technological applications [1–5]. The control of the characteristics (shape, size, orientation and periodicity) of such Laser Induced Periodic Surface Structures (LIPSS) has been boosted by the advent of ultra-short lasers (particularly femtosecond lasers). In addition to the Low Spatial Frequency LIPSS (LSFL) whose periodicity is typically very close to the laser wavelength, femtosecond lasers also permit the formation of High Spatial Frequency LIPSS (HSFL). These latter have a periodicity that is significantly lower than that of LSFL thus widening the range of different topologies that can be formed at the surface of a material through laser irradiation. Furthermore, there has been growing interest in the investigation of LIPSS formation on materials in thin film form [6,7] (as opposed to bulk material) in view of the ever-growing applications of thin films and coatings in a wide variety of industrial domains such as aerospace, medicine, electronics and optics. For thin films, LIPSS formation brings additional challenges [8,9] that include the effect of interfacial stresses between film and substrate, cavitation, physical properties of the

underlying substrate as well as the crystalline properties of the films that often depends on its initial elaboration.

In this paper, we present a comparative study of the formation of LIPSS using a femto-second laser on thin films titanium oxide (TiO_x) synthesized by Pulsed Laser Deposition (PLD) and Magnetron Sputtering (MS). This material was selected because of its wide applications in devices for harvesting energy (photo-voltaics, photo-catalyst) as well as its good stability at high temperature and its low negative environmental impact [10]. The effect of laser fluence and laser scanning parameters on the properties of the LIPSS were investigated using two different femtosecond laser sources and compared for both types of films (i.e. PLD and MS).

2. Experimental

Two deposition techniques, namely Pulsed Laser Deposition (PLD) and Magnetron Sputtering (MS) were used to grow titanium oxide thin films with typical thicknesses ranging between 300 and 500 nm on 1.2 μm thick SiO₂ layers thermally grown on Si (1 0 0) substrates. For the PLD experiments, a KrF excimer laser beam (248 nm, 10 Hz) was focused onto a stoichiometric ceramic TiO₂ target placed at a distance

* Corresponding author.

E-mail address: nadjib.semmar@univ-orleans.fr (N. Semmar).

of 50 mm from a heated substrate holder, under a 10^{-6} mbar vacuum base pressure. Film growth was performed on the conventionally cleaned substrates at a laser fluence of 4 J/cm^2 whereas the substrate was set at 700°C in order to induce a better film crystallinity. Under these experimental growth conditions, the homogeneous films were synthesized over an area of $1 \times 1 \text{ cm}^2$. They were found to be sub-stoichiometric with a ratio of O/Ti ranging from 1.6 to 1.8, as determined by Rutherford Backscattering Spectrometry (RBS) [11]. For the MS deposition runs, a 10 cm diameter and 4.0 mm thick titanium metallic target (Purity 99.995%) was magnetron sputtered in a pulsed DC mode using a mixture of Ar and O_2 gas. Details of the sputtering system are available elsewhere [12]. Film growth was thus achieved on unheated rotating substrate holder placed at a distance of ~ 127 mm from the target at a total pressure of 1 Pa (base pressure of $\sim 10^{-5}$ Pa). The flow rates of argon and oxygen were fixed at 20 and 1.5 sccm, respectively. Under these conditions, homogenous (over an area of $5 \times 5 \text{ cm}^2$) titanium oxide thin films with a Ti/O ratio of 1.8, is also determined by RBS.

The first set of experiments to micro/nanostructure the PLD and MS grown TiO_x thin films was performed using a 100 fs linearly polarized Ti: Sapphire laser emitting at 800 nm and operating at a repetition rate of 1 kHz. The laser spot diameter was focused to $350 \mu\text{m}$ on the surface of the films. The third harmonic at 266 nm, generated by tripling the frequency of the laser beam utilizing a BBO crystal, was used for these experiments, with a pulse duration of 100 fs. Treatment of large surfaces was accomplished by fixing the samples and a mirror reflecting the laser beam onto the sample was controlled by an x-y-translation device taking into account the laser pulse number by adjusting the translation step and working at a scan speed of 50 mm/s. More detailed information about these experimental parameters can be found in Talbi et al. [13]. Additional laser irradiation experiments were also performed on the MS films only using a Yb:YKW 500 fs linearly polarized laser emitting at 1030 nm that can operate at a repetition rate up to 300 kHz. An irradiation configuration similar to the one using for the Ti-sapphire laser was used, but at a scan speed of 4 mm/s and a repetition rate of 100 kHz. The beam waist in this case was determined to be $32 \mu\text{m}$, as estimated using the Liu method [14].

3. Results and discussion

Fig. 1 represents SEM images of $\text{TiO}_{1.8}$ thin films deposited on SiO_2 using (a) PLD and (b) MS. The surface morphology of the PLD film appears very smooth with a barely distinguishable nano-grained structure. This contrasts with a very obvious granular structure of the MS films and a rougher surface than their PLD counterparts. Cross-sectional SEM images (not shown) indicate a columnar growth in both cases, so the difference in surface morphology could be due to surface mobility effects of the incident species during film growth. Indeed, the kinetic energy species in the laser ablation plume are typically greater than that of sputtering species (in the absence of electrical bias of the substrate, as is the case here). Furthermore, the PLD films were grown at a substrate temperature of 700°C whereas the MS films were not heated during growth (a substrate temperature increase of no more than 50°C would be expected though). This difference in growth temperature could also explain the difference in surface roughness between the PLD and the MS films.

Fig. 2 show SEM images of the (a) PLD and (b) MS TiO_x films after irradiation with the 266 nm wavelength laser at a fluence of 15 mJ/cm^2 and a number of pulses of 13000. The number, N , of pulses received by each point of film surface is given by the following relationship:

$$N = \left(\frac{d}{s}\right)^2$$

where d is the spot diameter and s is the step of translation along the x-axis or y-axis [13]. The SEM images for both samples, whether

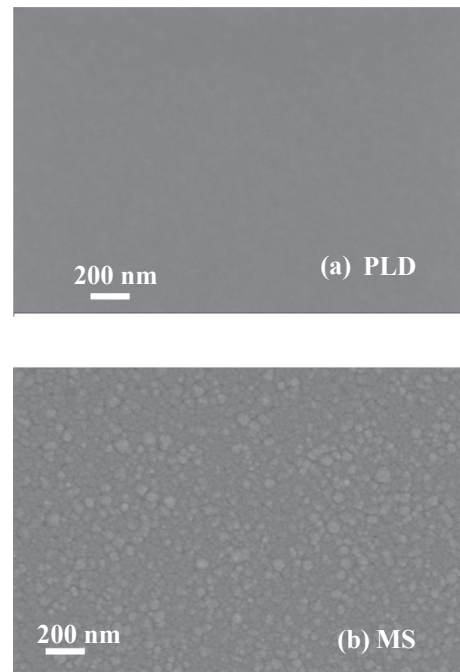


Fig. 1. SEM images of TiO_x thin films deposited by (a) PLD and (b) MS.

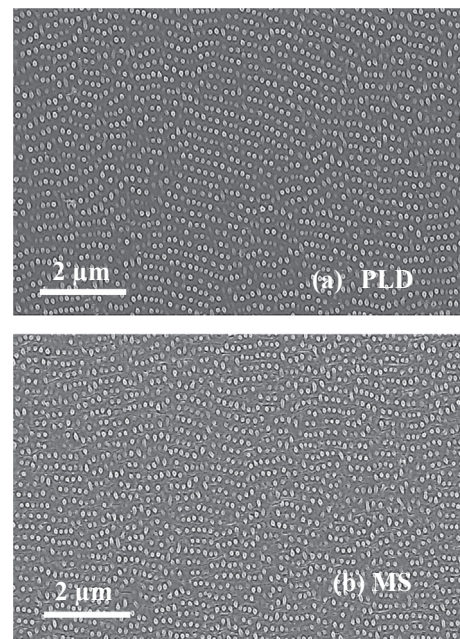


Fig. 2. SEM images of (a) PLD and (b) MS TiO_x films irradiated by 100 fs laser pulses at a wavelength of 266 nm with $F = 15 \text{ mJ/cm}^2$ and $N = 13,000$.

deposited by PLD or MS, show that laser irradiation under these conditions lead to the formation of regularly spaced dots with two periods at 266 and 160 nm, the latter being nearly half of the laser wavelength. Typical heights of these dots were estimated at 40 nm by preliminary Atomic Force Microscopy (AFM) measurements. These periods could be considered as LSFL and HSFL respectively, but the patterns are wavy and do not strictly follow a direction that is either parallel or perpendicular to the beam polarization. This effect is probably due to the overlap of the successive beams. These patterns are similar to those obtained under static beam conditions (one laser spot without scanning) and were mainly attributed to a self-organization process. In such a process, the melting of the surface layers can be induced by the ultra-

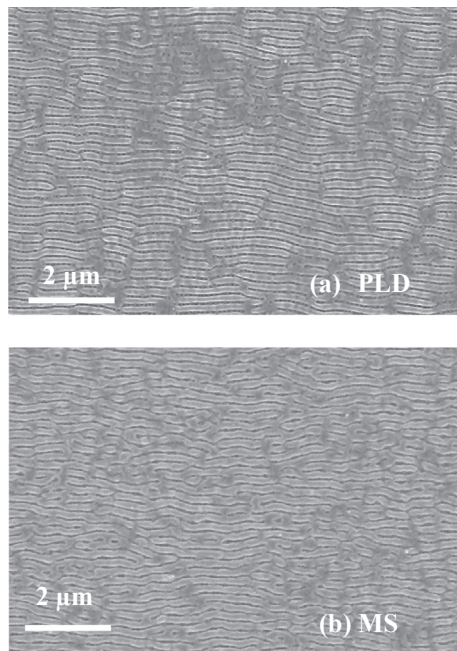


Fig. 3. SEM images of (a) PLD and (b) MS TiO_x films irradiated by 100 fs laser pulses at a wavelength of 266 nm with $F = 25 \text{ mJ/cm}^2$ and $N = 33,000$.

short laser pulse at UV wavelength, where material absorption is high and depth penetration is low. Melted material would then agglomerate in regular dots as a result of surface energy minimization [15].

In a previous paper [13], it has been shown varying laser fluence and number of pulses can lead to a variety of different surface morphologies ranging from dots to LSFL, HSFL as well as intermediate morphologies. Thus, PLD and MS films were irradiated under different conditions, as seen in Fig. 3, namely at a fluence of 25 mJ/cm^2 and a total number of pulses of 3300. The obtained morphology consists of LSFL with a period of $\sim 240 \text{ nm}$ and an orientation predominantly parallel to the beam polarization. Careful observation of the LSFL shows that there are some locations where a “linking” between the LSFL occurs. The presence of such links or bridges supports the self-organization model [4] where there is evolution of the surface from regularly spaced dots to LSFL with increasing laser fluence. Comparing the images of the PLD films (Fig. 3a) and those of the MS films (Fig. 3b), it is also clear that the formed patterns are quite similar quantitatively (very close spatial period of the LSFL- and HSFL-LIPSS as determined above) and qualitatively (shape/type of the LIPSS, dots or lines, depending on laser irradiation conditions). Further increase in laser fluence, up to 30 mJ/cm^2 for a number of pulses of 13,000 leads to a destruction of the previously described nanostructures through a dominant ablation-evaporation process, again for both PLD and MS films. However, despite these very similar results obtained within the experimental conditions used in this work, the delamination of the MS thin films is noticed in some zones of the treated surface for a laser dose of 25 mJ/cm^2 and 3300 pulses (as seen in Fig. 4). Such delamination effects were not observed for the PLD films. The delamination of a thin film under laser irradiation can be a result of ablation phenomena induced through a thermo-mechanical process [16,17]. It is clear from Fig. 4 that, after film delamination, the substrate surface appears very clean without any damage and the delaminated film exhibits the regular LSFL pattern, inferring that the delamination occurs after or simultaneously to the LSFL formation. It is also noteworthy through observation of the delaminated layers in Fig. 4 that the amplitude of the LIPSS pattern is much less than the thickness of the film. We can thus conclude that de-wetting of the substrate essentially plays no role in the LIPSS formation. Since, no such delamination was observed in the case of PLD thin films, it can be concluded that the adhesion and thermo-

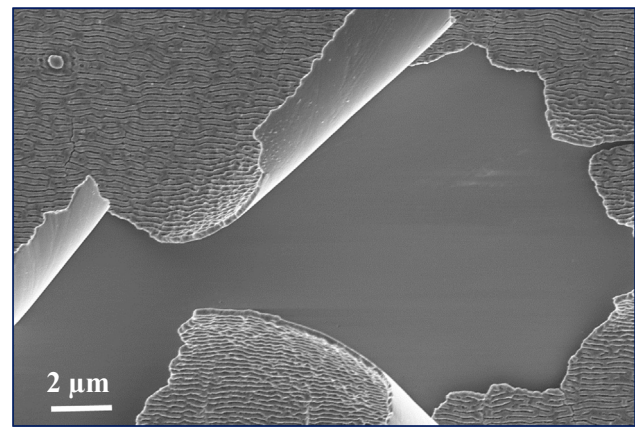


Fig. 4. SEM image of a delamination observed on a MS by film irradiated 100 fs laser pulses at a wavelength of 266 nm.

mechanical properties of the latter films on the substrate are better than their MS counterparts. This could be attributed to the nature of the PLD process whereby the highly energetic particles present in the ablation plume and impinging on the substrate and on the film as it grows, can enhance surface adhesion on the substrate. Furthermore, high internal compressive stress is expected to be present in the MS films because they were grown at room temperature, which is not the case of the PLD films. Yet, the delamination of the MS films occurs only after laser irradiation. It is widely accepted in literature that, the cracking, fragmentation and delamination of material occurs due to the thermo-elastic stresses induced by laser irradiation [16–18]. As result of the femtosecond pulse, the laser energy absorption causes a confined heat in the irradiated volume. This thermal confinement leads to an increasing temperature within the irradiated zone leading to thermo-elastic stress [17]. Due to the repeated rapid heating/cooling processes, a very high density of such thermo-elastic stress can be generated which causes the fracture by fatigue and delamination of the layers.

In order to further investigate the effect of laser fluence on the delamination of MS films and with the aim of nano-structuring large areas of the films ($2.5 \times 2.5 \text{ cm}^2$), MS films were irradiated using the 500 fs laser emitting at 1030 nm expecting a lower peak power. The repetition rate, the scan speed and the spacing between lines were fixed to respectively 100 kHz, 4 mm/s and $5 \mu\text{m}$ leading to a number of pulses of 24,000. This much higher frequency of the laser (100 kHz) compared to the previous one (1 kHz) allowed irradiation of large area within a reasonable period of time (tens of minutes). Fig. 5 shows the effect of surface morphology of MS films following irradiation at different values of laser fluence, ranging from 55 to 220 mJ/cm^2 . These fluences exceed the surface damage threshold which was estimated at 36 mJ/cm^2 after 10,000 pulses under static laser irradiation i.e. with no beam scanning. The damage threshold was deduced by SEM observation of the damage zone expansion as the number of pulses is increased under static laser irradiation. A somewhat unexpected behavior of surface morphology evolution is observed, with increasing laser fluence. Indeed, for fluences ranging from 55 to 85 mJ/cm^2 , film delamination is severe but the effect appears to be drastically reduced by for a fluence of 110 mJ/cm^2 and higher, and a micro-cracked surface morphology is observed. A schematic showing the different damage threshold fluences for a Gaussian laser beam profile (as is the case for the 500 fs laser) is illustrated in Fig. 6. This schematic can be used to explain the effects seen in Fig. 5, through the following mechanisms. The surface of the film can be damaged through two main processes: (1) Cracks and delamination processes induced by thermo-elastic stresses (2) Ablation, evaporation and melting processes induced by the lattice heating due to heat accumulation. Assuming that, after multiple shots, the cracking (stress) threshold is lower than thermal threshold (melting), F the applied fluence is greater than the cracking (stress) threshold but lower than the

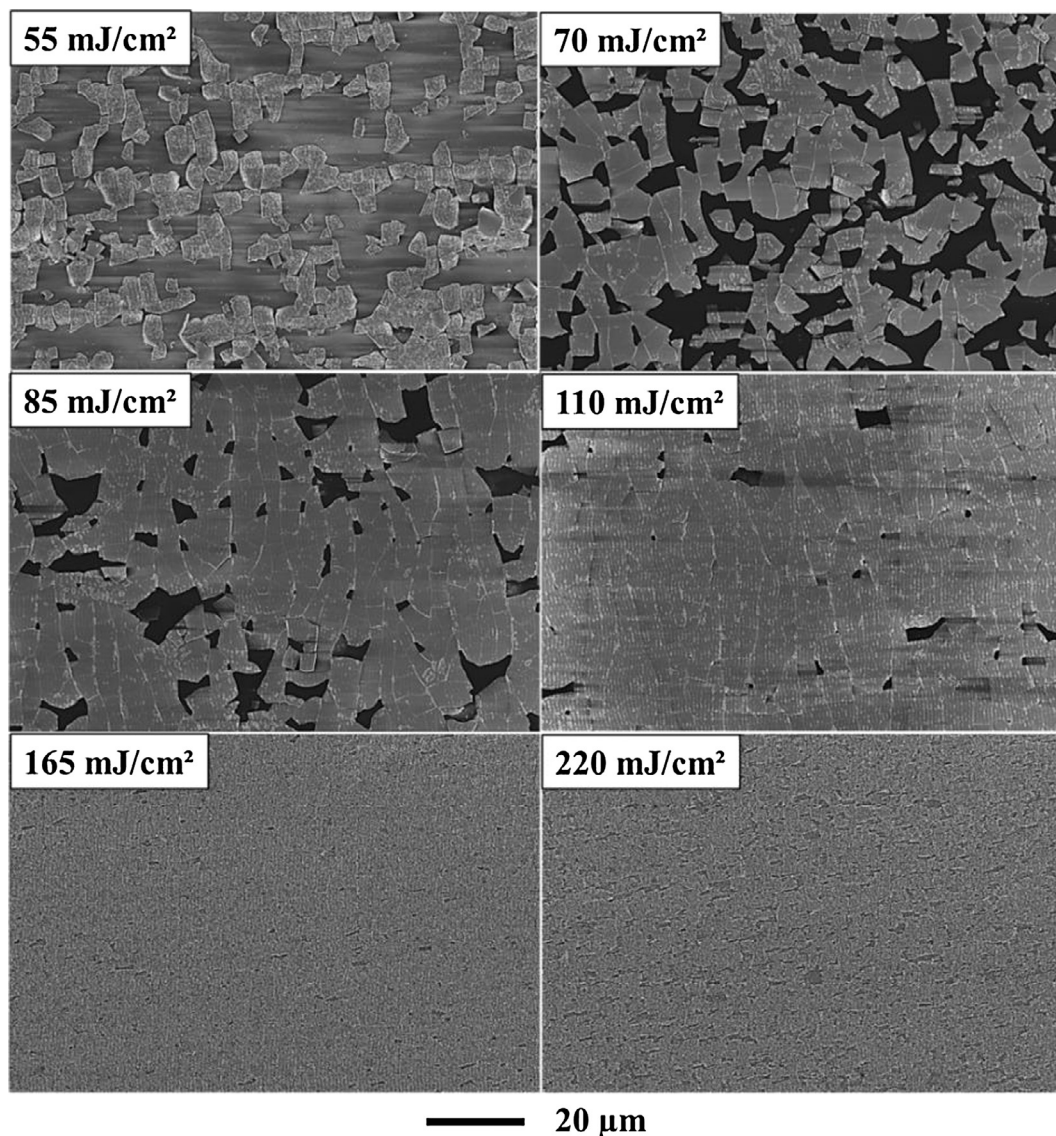


Fig. 5. SEM images of TiO_x MS films irradiated at 1030 nm at different laser fluences for $N = 24,000$.

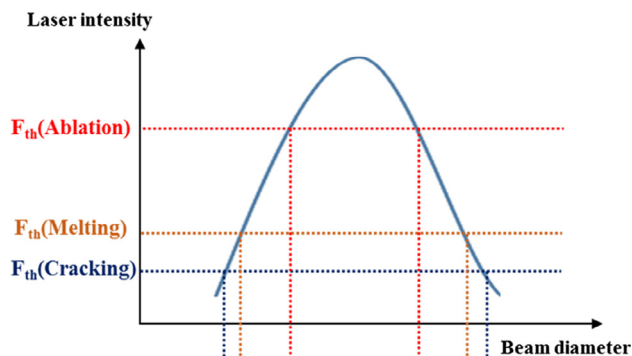


Fig. 6. Schematic showing the different damage threshold fluences for a Gaussian laser beam profile.

ablation (evaporation and melting) threshold, laser irradiation can lead to significant film damage manifested through cracking and delamination processes in form of flakes (in our case, this would correspond to laser fluences lower than 110 mJ/cm^2). On the other hand, if the applied fluence is above the melting and cracking threshold fluence but does not exceed the ablation (evaporation) threshold, the laser

irradiation would induce thermo-elastic stresses leading to the generation of cracks, while simultaneously triggering a melting process. This latter can lead to stress relaxation and induce “repair” of the surface damage induced by cracks and delamination. This proposed mechanism as well as LIPSS formation under femto-second laser irradiation of MS films at a wavelength of 1030 nm will be the subject of future work.

4. Conclusion

In this paper, we present a comparative study of LIPSS formation on sub-stoichiometric titanium oxide thin films (TiO_x , with $1.6 \leq x \leq 1.8$) that were grown using two different techniques, namely pulsed laser deposition (PLD) and magnetron sputtering (MS). Irradiation was performed using femtosecond lasers beams, emitting at wavelengths 266 and 1030 nm, and at different number of laser pulses and laser fluences. Conditions for the formation of LIPSS were determined for both types of films, at 266 nm. A variety of nanostructures such as LSFL, HSFL, spikes, dots were detected and their shapes and sizes were found to strongly depend on laser fluence and number of pulses, as essentially dictated by free-surface energy minimization. LIPSS appeared to follow similar formation pattern for both PLD and MS films, except for some

delamination detected for the MS films. This was attributed to better adhesion and lower internal stress of the PLD films compared to their MS counterparts. Large surface nanostructuring experiments performed at 1030 nm showed less delamination with the increase of the laser fluence, a phenomenon attributed to the competition between the cracking and the melting processes of the layers.

Acknowledgements

This project was supported through a French National project 'Projet Investissement d'Avenir - Tours2015' in collaboration with STMicroelectronics in Tours. MT would like to thank the University of Orléans and the SAFAR program for a financial support during the completion of this work.

References

- [1] J. Bonse, H. Sandra, S.V. Kirner, A. Rosenfeld, J. Krüger, Laser-induced periodic surface structures — a scientific evergreen, *IEEE J. Select. Top. Quant. Elect.* 23 (3) (2017) 9000615.
- [2] M. Ahn, R. Cahyadi, J. Wendorf, W. Bowen, B. Torralva, S. Yalisove, J. Phillip, Low damage electrical modification of 4H-SiC via ultrafast laser irradiation, *J. Appl. Phys.* 123 (2018) 145106.
- [3] A.Y. Vorobyev, C. Guo, Direct femtosecond laser surface nano/microstructuring and its applications, *Laser Photonics Rev.* 7 (3) (2013) 385–407.
- [4] J. Reif, O. Varlamova, S. Uhlig, S. Varlamov, M. Bestehorn, On the physics of self-organized nanostructure formation upon femtosecond laser ablation, *Appl. Phys. A Mater. Sci. Process.* 117 (1) (2014) 179–184.
- [5] E.L. Gurevich, S.V. Gurevich, Laser Induced Periodic Surface Structures induced by surface plasmons coupled via roughness, *Appl. Surf. Sci.* 302 (2014) 118–123.
- [6] K. Bobzin, T. Brögelmann, A. Gillnerb, N.C. Kruppe, C. Heb, M. Naderi, Laser-structured high performance MS coatings, *Surf. Coatings Technol.* 352 (2018) 302–312.
- [7] E. Rebollar, M. Castillejo, T.A. Ezquerro, Laser induced periodic surface structures on polymer films: from fundamentals to applications, *Eur. Polym. J.* 73 (2015) 162–174.
- [8] M. Zamfirescu, A. Dinescu, M. Danila, G. Socol, C. Radu, The role of the substrate material type in formation of laser induced periodical surface structures on ZnO thin films, *Appl. Surf. Sci.* 258 (2012) 9385–9388.
- [9] M. Hashida, Y. Miyasaka, Y. Ikuta, S. Tokita, S. Sakabe, Crystal structures on a copper thin film with a surface of periodic self-organized nanostructures induced by femtosecond laser pulses, *Phys. Rev. B* 83 (2011) 235413.
- [10] X. Chen, S.S. Mao, Titanium dioxide nanomaterials: synthesis, properties, modifications, and applications, *Chem. Rev.* 107 (2007) 2891–2959.
- [11] E. Le Boulbar, E. Millon, J. Mathias, C. Boulmer-Leborgne, M. Nistor, F. Gherendi, N. Sbaï, J.B. Quoirin, Pure and Nb-doped TiO_{1.5} films grown by pulsed-laser deposition for transparent p-n homojunctions, *Appl. Surf. Sci.* 257 (12) (2011) 5380–5383.
- [12] P. Coddet, J. Vulliet, C. Richard, A. Caillard, A.L. Thomann, Characteristics and properties of a magnetron sputtered gadolinia-doped ceria barrier layer for solid oxide electrochemical cells, *Surf. Coat. Technol.* 339 (2018) 57–64.
- [13] A. Talbi, C.T. Tameko, A. Stolz, E. Millon, C. Boulmer-Leborgne, N. Semmar, Nanostructuring of titanium oxide thin film by UV femtosecond laser beam: From one spot to large surfaces, *Appl. Surf. Sci.* 418 (2017) 425–429.
- [14] J.M. Liu, Simple technique for measurements of pulsed Gaussian-beam spot sizes, *Optics Letters* 7 (5) (1982) 1980–1982.
- [15] T.T.D. Huynh, M. Vayer, A. Sauldubois, A. Petit, N. Semmar, Evidence of liquid phase during laser-induced periodic surface structures formation induced by accumulative ultraviolet picosecond laser beam, *Appl. Phys. Lett.* 107 (2015) 193105.
- [16] J. Lee, S. Kim, M. Lee, Micro-scale patterning of indium tin oxide film by spatially modulated pulsed Nd:YAG laser beam, *Appl. Surf. Sci.* 258 (23) (2012) 9107–9111.
- [17] N. Farid, H. Chan, D. Milne, A. Brunton, G.M.O. Connor, Stress assisted selective ablation of ITO thin film by picosecond laser, *Appl. Surf. Sci.* 427 (2017) 499–504.
- [18] G.M.O. Connor, C. McDonnell, D. Milne, C. Prieto, H. Chan, D. Rostohar, G.M.O. Connor, Laser patterning of very thin indium tin oxide thin films on PET substrates, *Appl. Surf. Sci.* 359 (2015) 567–575.